Available online at www.sciencedirect.com
SCIENCE DIRECT
Polymer 46 (2005) 12480–12492
polymer
www.elsevier.com/locate/polymer

Fracture toughness of polymers in shear mode

H.J. Kwon *, P.-Y.B. Jar

Department of Mechanical Engineering, University of Alberta Edmonton, AB, Canada T6G 2G8

Received 8 August 2005; received in revised form 13 October 2005; accepted 14 October 2005
Available online 3 November 2005

Abstract

This paper presents a new test method that measures fracture toughness of polymeric materials when subjected to in-plane shear loading (mode II), and compares the toughness with that in tension mode (mode I). The new test method uses an Iosipescu device to apply the shear load, and determines the toughness based on the concept of essential work of fracture (EWF). Three physical-based criteria were used to verify the occurrence of mode II fracture. The new test method was then used to evaluate toughness of poly(acrylonitrile–butadiene–styrene) (ABS). The results suggest that for the ABS, the ratio of toughness in mode II to mode I is about 2.5 which leads to the dominance of mode I fracture in most loading conditions. The results also showed that for ABS in mode I fracture, the specific work of fracture (defined as the absorbed energy for fracture divided by the cross sectional area of the ligament between the notch tips) depends on ligament length; while in mode II fracture, it depends on ligament thickness. The study concludes that the new test method has a good potential for evaluation of mode II fracture toughness of polymers, though further study using polymers of different characteristics will be needed to confirm universality of the test method in the measurement of mode II fracture toughness.

Keywords: Shear fracture; Toughness; EWF

1. Introduction

Toughness, a measure of resistance to fracture, has long been evaluated for polymeric materials using concepts such as stress intensity factor (K_c), energy release rate (G_c), J-integral (J_c), etc. Test methods developed using these concepts are based on linear elastic fracture mechanics (LEFM) approach, originally developed for brittle materials, that is, they are normally used when linear elasticity dominates the deformation behaviour and the plastic deformation is limited to the vicinity around the crack tip. Validity of this principle, however, has been questioned when considered for toughness measurement of ductile materials in which the fracture is accompanied with significant plastic deformation. Furthermore, current methods have difficulties in measuring toughness of polymers in shear mode (mode II). The reason, as Williams [1] stated, is that most polymers have much lower toughness in tension mode (mode I) than that in shear mode (mode II). Therefore, global failure behaviour of polymers in most load-bearing structures is believed to be in mode I even though in the initiation stage the behaviour can be in a shear-like mode [2,3]. Since current testing methods are not suitable for the measurement of mode II fracture toughness, especially for ductile polymers, no experimental data are available to support the above statement. The lack of testing method to measure mode II fracture toughness also hinders the capability of failure analysis in loading scenarios that involve mainly shear forces.

A relatively new test method based on the concept of essential work of fracture (EWF) [4] was proposed to characterize fracture toughness of ductile materials. The EWF concept was firstly proposed by Broberg [5,6], and has been accepted widely as a means to quantify fracture toughness of ductile materials in the sheet form where the deformation occurs in the plane-stress conditions. Up to now, most studies using the EWF concept have been limited to mode I fracture [7,8] and some special cases of mode III fracture [9]. The EWF concept is yet to show the applicability to the measurement of mode II fracture toughness.

The purpose of this study is to establish a testing method, based on the EWF concept, to evaluate mode II fracture toughness of polymeric materials. The testing method uses Iosipescu loading to apply a shear force [10,11] in the middle section of the specimen where edge notches are machined on both sides of the specimen. In addition to the notches, grooves were introduced along the specimen surfaces between the notch tips to encourage fracture in a direction parallel to the

* Corresponding author. Tel.: +1 780 492 6503; fax: +1 780 492 2200.
E-mail address: hkwon@ualberta.ca (H.J. Kwon).

0032-3861/$ - see front matter © 2005 Elsevier Ltd. All rights reserved.
doi:10.1016/j.polymer.2005.10.074

shear force, thus the mode II fracture. This paper firstly provides the background knowledge for the development of the new test method for mode II fracture, and then presents some experimental evidence on the mode II fracture toughness for a rubber-modified polymer and the associated deformation behaviour.

2. Theoretical analysis

2.1. Review of fracture analysis using classical LEFM

Most criteria for material fracture are based on LEFM, under the assumption that crack extension is governed by a specific fracture parameter, such as stress, strain, or energy. Three common criteria used in the past are maximum circumferential stress [12], maximum strain energy release rate [13], and minimum strain energy density [14]. For two-dimensional cases, stress intensity factors (K_1 and K_2) are used to estimate the stress amplification at certain point away from the crack tip, which are defined as $K_1(\theta) = \lim_{r\to 0}(\sigma_\theta\sqrt{2\pi r})$ for mode I, and $K_2(\theta) = \lim_{r\to 0}(\tau_{r\theta}\sqrt{2\pi r})$ for mode II, where σ_θ and $\tau_{r\theta}$ are circumferential normal and shear stresses, respectively, in polar coordinates in the singularity dominated zone [15]. For example, under pure tensile loading, using the criterion of maximum circumferential stress, it has been shown that $K_{1(\max)} = \sigma\sqrt{\pi a}$ along $\theta_0 = 0°$ and $K_{2(\max)} = 0.38\sigma\sqrt{\pi a}$ along $\theta_0 = 70.5°$ where θ_0 is the angle of crack propagation with respect to the original crack orientation, and σ the remote tensile stress. Similarly, under pure shear loading $K_{2(\max)} = 0.866\tau\sqrt{\pi a}$ along $\theta_0 = 0°$ while $K_{1(\max)} = \tau\sqrt{\pi a}$ along $\theta_0 = -70.5°$ where τ is the remote shear stress. Fig. 1 depicts the variations of the normalized $K_1(\theta)$ and $K_2(\theta)$, by dividing K_1 and K_2 by $\sigma\sqrt{\pi a}$ and $\tau\sqrt{\pi a}$, respectively, where σ and τ are the applied normal and shear stresses. The curves in Fig. 1 show that $K_{1(\max)}$ is always greater than $K_{2(\max)}$. Other conditions such as mixed tension–shear or compression–shear loadings give similar results, i.e. $K_{2(\max)} < K_{1(\max)}$. Therefore, in terms of stress intensity factor generated by the applied load, mode I is the preferred mode of fracture. Similar conclusions can be drawn from other fracture criteria, such as strain energy release rate, and have been verified using finite element (FE) modeling [16]. For polymers, the critical stress intensity factor in mode II (K_{IIC}) is expected to be much larger than that in mode I (K_{IC}) [1]. Therefore, in terms of material properties (critical stress intensity factor) mode I also dominates fracture in most polymers.

It should be noted that local yielding mode can be very different from global fracture mode. Since shear strength for some polymers are lower than their tensile strength [3,17], shear type cracking can occur at the yielding and crack initiation stage [2] in cases that the ratio of the applied shear stress to tensile stress is high. However, the subsequent fracture mode may switch to mode I as the crack and the accompanied plastic deformation zone evolve. This is because most polymers have higher fracture toughness in mode II than in mode I. As a result, it is believed that the global crack development process is dominated by mode I fracture; while the crack initiation can occur in shear mode.

The LEFM approach is known to have limited validity when extensive plastic deformation is accompanied with fracture or when fracture toughness needs to be evaluated beyond the crack initiation stage. One way to overcome the problem is to use the concept of essential work of fracture (EWF) to quantify the toughness, as to be discussed in the following section.

2.2. Review of essential work of fracture (EWF)

The EWF concept is to extract the energy for the formation of crack surface from the total energy absorbed in the fracture process. The basic requirement of the EWF concept is that the ligament between two edge cracks, L_0 in Fig. 2, should yield completely before fracture occurs, but the plastic deformation should be confined to regions around the ligament. Therefore, the energy absorbed for the formation of crack surface is determined by extrapolating the value of energy absorption per unit crack area to the case with zero ligament length, as the corresponding energy for plastic deformation is zero.

Using the EWF concept, work provided to fracture the specimen can be divided into two parts: (i) the work for plastically deforming the region around the ligament, which is

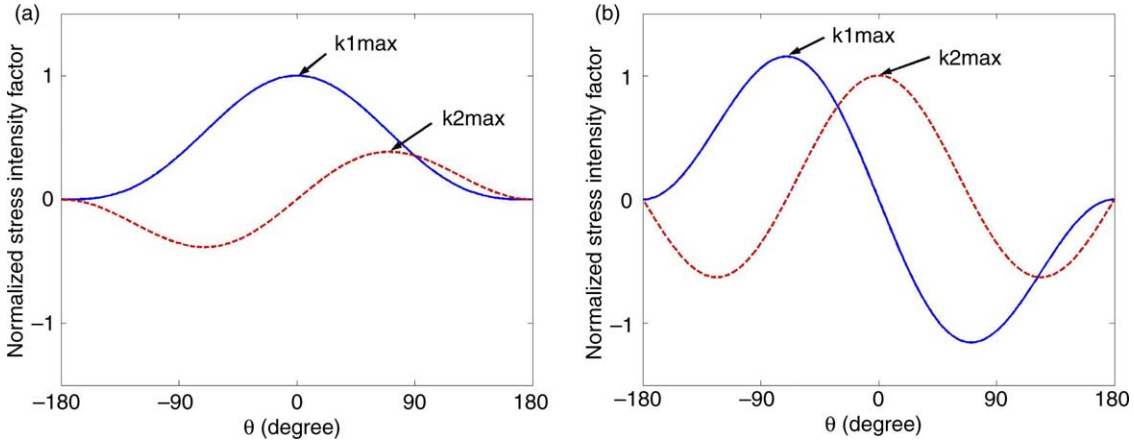

Fig. 1. Normalized variation of $K_1(\theta)$ (—) and $K_2(\theta)$ (– – –) with respect to θ: (a) under mode I (tensile) loading, and (b) under mode II (shear) loading.

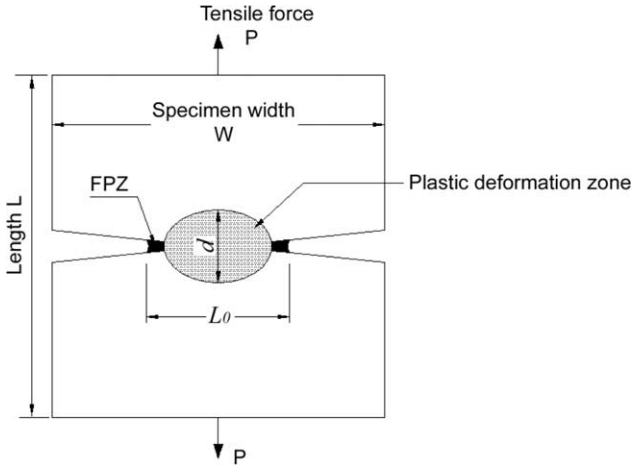

Fig. 2. Double-edge-notched (DEN) tensile specimen for mode I fracture.

expected to be proportional to the volume of plastic deformation zone provided that full plastic deformation is developed before crack growth commences, and (ii) the essential work required for the formation of fracture surface, which is proportional to the cross sectional area of the ligament. Value of EWF has been found to increase with the increase of specimen thickness due to localized necking [18]. The width of the plastic deformation zone, d in Fig. 2, on the other hand, is known to be proportional to initial ligament length, L_0. Therefore, the total work of plastic deformation, W_p^I, is proportional to L_0^2. As a result, the total work of fracture, W_f^I, can be expressed as the sum of the essential work of fracture (W_e^I), the work for the necking (W_n^I), and the work for plastic deformation (W_p^I):

$$W_f^I = W_e^I + W_n^I + W_p^I = \Gamma_0^I L_0 t_0 + \beta_1 w_n^I L_0 t_0^2 + \beta_2 w_p^I t_0 L_0^2 \quad (1)$$

where t_0 is the initial thickness, Γ_0^I the specific essential work of fracture in mode I, w_n^I the average work density for the neck forming, w_p^I the average plastic work density, and β_1 and β_2 the shape factors for the neck and the plastic deformation zone, respectively. By measuring the total work of fracture for specimens of different thickness and ligament lengths, and dividing the total work of fracture by the ligament cross sectional area ($L_0 \times t_0$) using specimens with geometry depicted in Fig. 2, the specific work of fracture, w_f^I, can be expressed in terms of Γ_0^I, w_n^I and w_p^I as:

$$w_f^I = \Gamma_0^I + \beta_1 w_n^I t_0 + \beta_2 w_p^I L_0 = w_e^I + \beta_2 w_p^I L_0 \quad (2)$$

The first term in the very right expression, w_e^I, is a combinations of Γ_0^I and $\beta_1 w_n^I t_0$, i.e. $w_e^I = \Gamma_0^I + \beta_1 w_n^I t_0$, which is known as the specific essential work of fracture for a given thickness.

The EWF concept has made a great success in measuring toughness of metal plates. As a result, interests have increased tremendously in last few years in applying the EWF concept to evaluate toughness of polymer plates. However, as mentioned earlier, its current applications are limited to mode I fracture and special cases of out-of-plane tearing (mode III fracture). Very few studies have been reported on the use of the EWF concept to characterize the toughness in mode II fracture, except one study on metallic plates [19] for which mode II is known to be the preferred mode of fracture.

2.3. Velocity discontinuity in plastic deformation zone

During the plastic deformation, velocity field in a plate specimen may show an abrupt change in a very narrow region, known as velocity discontinuity [20] that leads to thickening or thinning of the region. Hill [21] considered the velocity discontinuity for the neck forming process in a plate that is subjected to plane-stress deformation, and correlated the velocity discontinuity with the strain rate in the necking process. For an idealized neck that is subjected to a uniform strain rate, as shown in Fig. 3, with the region on the right-hand side of the neck moving at a velocity v relative to the left-hand side, the strain-rate components that are tangential and normal to the neck, i.e. $\dot{\varepsilon}_{tt}$, $\dot{\varepsilon}_{nt}$ and $\dot{\varepsilon}_{nn}$, can be expressed as:

$$\dot{\varepsilon}_{nn} = \frac{v_n}{b} = \frac{v}{b}\sin\gamma, \quad \dot{\varepsilon}_{tt} = 0, \quad \text{and} \quad \dot{\varepsilon}_{nt} = \frac{v_t}{b} = \frac{v}{b}\cos\gamma \quad (3)$$

where b is the width of the neck, γ the angle between velocity v and the neck, and v_n and v_t normal and tangential components of v, respectively. When pure mode II fracture occurs, the neck should have negligible width ($b \approx 0$) and the two halves in Fig. 3 are expected to move relative to each other in a sliding mode, i.e. $\gamma = 0$.

2.4. The proposed EWF analysis for mode II fracture

In addition to the limited deformation, the classical fracture mechanics does not clearly distinguish the loading mode from the deformation or fracture mode. For the three fundamental modes of fracture, i.e. tension, in-plane shear and out-of-plane tearing (i.e. mode I, II and III, respectively), the underlined assumption in the classical fracture mechanics is that the crack growth direction (at the macroscopic level) is associated with the loading mode. This, however, is well known to fail in many polymers when subjected to mode II loading, as mode I fracture usually occurs at the crack tip due to their low mode I fracture toughness value. To resolve the inconsistency between the loading mode and the fracture mode, it is proposed here that the mode of fracture should be considered independently from

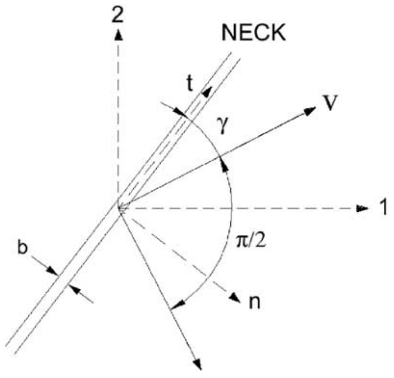

Fig. 3. Velocity discontinuity.

the mode of loading. In other words, the loading mode should not be used as a criterion to identify the fracture mode, and it is possible that a fracture mode may occur in any loading mode. Therefore, the mode II fracture toughness should be measured when mode II fracture occurs, not when mode II loading is applied.

Without the loading mode to serve as a criterion, other criteria are needed to identify the mode II fracture. At the microscopic level, the crack growth in mode II fracture is expected to be in a direction parallel to the fracture surface and perpendicular to the crack front, which is known to hardly occur in amorphous polymers. An example is given by O'Brien [22] who observed the formation of 'hackles' in a resin-rich layer of fibre-reinforced polymers (FRP) that had been subjected to mode II loading. He suggested that the hackles were a result of formation and coalescence of micro-cracks that were not parallel to the global fracture surface, and concluded that the mode II fracture which consists of the sliding of one plane relative to another does not occur locally at the crack tip. Numerous other studies also showed that polymers do not deform and fracture in mode II at the microscopic level. Since most polymers do not deform in mode II microscopically, we proposed the following criteria, based on the fundamental concept of the expected deformation behaviour, to identify mode II fracture of polymers.

(i) *Crack orientation*: in the aforementioned classical fracture mechanics [12 – 14], the macroscopic crack orientation in mode II fracture, when subjected to pure shear loading, should be parallel to the maximum shear stress.

(ii) *Development of fracture process zone (FPZ)*: the conventional definition of mode II fracture in a double-edge-notched specimen is that the fracture process should occur across the entire section between the two notches, i.e. the fracture process zone (FPZ) should be formed in the entire section prior to the crack evolvement, as shown in Fig. 4. This is different from the crack development in mode I fracture that has been shown in Fig. 2 in which the FPZs are limited at the notch tips [7,23] and progress towards each other as the crack grows.

(iii) *Work of fracture*: since the FPZ is formed across the entire ligament section uniformly, size of the plastic deformation zone should also be uniform in the ligament section, as shown in Fig. 4, and the total work for the plastic deformation, W_p^{II}, should be proportional to the cross sectional area of the ligament, $L_0 t_0$, instead of $L_0^2 t_0$ for the mode I fracture (Eq. (1)). Under this condition, the total work of fracture, W_f^{II}, for the mode II fracture can be expressed as:

$$W_f^{II} = W_e^{II} + W_p^{II} = w_e^{II} L_0 t_0 + \beta_3 w_p^{II} L_0 t_0 \quad (4)$$

where W_e^{II} is the essential work of fracture, w_e^{II} the specific essential work of fracture for a given thickness, β_3 a shape factor, w_p^{II} the average plastic work density, and superscript 'II' represents mode II fracture. The corresponding specific work of fracture, w^{II}, is:

$$w_f^{II} = w_e^{II} + \beta_3 w_p^{II} \quad (5)$$

It should be noted that there is a possibility for w_f^{II} to be dependent on the specimen dimensions, similar to that shown by Eq. (2). Experiments have been conducted to elucidate such dependence, and the results will be shown later in this paper.

Eqs. (2) and (5) indicate that a significant difference exists between the expressions of the specific work of fracture w_f in mode I and mode II, especially as a function of the ligament length L_0. For the mode I fracture, the specific work of fracture w_f^I is proportional to the ligament length L_0; but for the mode II fracture, w_f^{II} should be independent of L_0. Experimental study, as to be shown later in this paper, has been carried out to verify this difference.

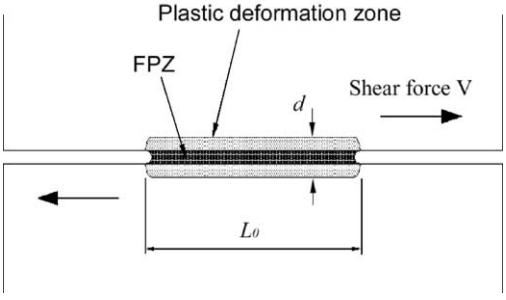

Fig. 4. Double-edge-notched (DEN) shear specimen for mode II fracture.

3. Experimental study

3.1. Material

Poly(acrylonitrile–butadiene–styrene) (ABS) that is known to have higher fracture toughness in mode II than in mode I was selected for the study. The ABS used was a commercially available extrusion grade in the plate form with nominal thickness of 6 mm, synthesized through emulsion polymerization. Rubber particle content is about 17%, with particle size below 1 μm. Preliminary tensile tests showed that the plates are isotropic in mechanical properties, with tensile strength close to 48 MPa and Young's modulus 2.5 GPa.

3.2. Mode I fracture toughness

The EWF test method used in Refs. [4,24,25] was adopted to measure the w_f^I value. Dimensions of double-edge-notched (DEN) specimens were 90 mm (width, W)×270 mm (total length, L) with varying thickness and ligament length. Tests were conducted using an Instron universal testing machine at a crosshead speed of 2.5 mm/min.

3.3. Mode II fracture toughness

Several test devices were considered to apply the shear force to ABS, including off-axis tensile test [26], Arcan test [27] and

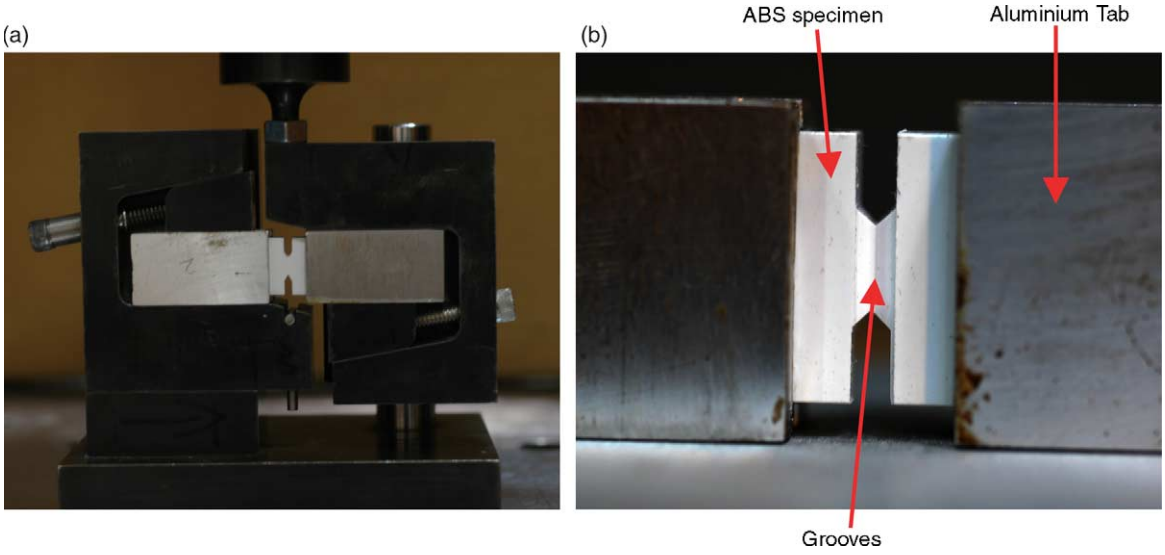

Fig. 5. Test set-up and specimens used in this study: (a) Iosipescu device and the specimen without grooves, and (b) the specimen with grooves.

Iosipescu shear test [28]. Among them, the Iosipescu test has relatively good precision in applying uniform pure shear force across the central cross section between the notches, thus being chosen for this study. Both sides of the specimens were bonded with aluminium tabs to minimize flexural deformation during the test.

The commonly used notch angles for Iosipescu specimens are either 90 or 110° [29,30] both of which were found to be improper for our test because these specimens could not avoid the generation of a secondary crack on the notch faces (details to be shown in Section 4.3). Instead, a reduced notch angle of 60° was selected for our study, and introduced to DEN specimens of 17 mm (W)×90 mm (L) with varying ligament length and specimen thickness. One study that used Iosipescu loading to measure mode II fracture toughness [31] chose single-edge-notched (SEN) specimen and J-integral method. However, due to asymmetric fracture behaviour in the SEN specimen the EWF concept cannot be applied to determine the fracture toughness.

In our study, V-shaped grooves were introduced to some of the specimens along the ligament section between the notch tips to enhance the alignment of the relative velocity with the direction of the ligament length. The Iosipescu device and the DEN specimen without the grooves are shown in Fig. 5(a) and the specimen with grooves in Fig. 5(b). Again, Instron universal testing machine at a cross-head speed of 2.5 mm/min was used for the test. Fracture behaviour was recorded using a digital video camera with a micro-zoom lens.

3.4. Fractography

A scanning electron microscope (SEM, JEOL JSM-6301F), a digital video camera, and a profile projector (Mitutoyo PH-3500) were used to record the fracture behaviour. Each specimen of interest for SEM was mounted on a sample holder and coated with a thin layer of gold just before the examination.

4. Results and discussion

4.1. Mode I fracture toughness

Preliminary results from mode I EWF test are summarized in Fig. 6, using specimens with ligament length in the range from 3 to 30 mm and thickness 6 mm. The data show a transition from pure plane-stress condition to mixed plane-stress and plane-strain conditions at the ligament length around 8 mm, as suggested in Ref. [32]. For ligament length in the range from 8 to 25 mm, the data show a linear variation between the specific work of fracture (w_f^I) and ligament length. Above 25 mm, the change of w_f^I and ligament length no longer followed a linear relationship. Therefore, the ligament lengths in the range from 8 to 25 mm were selected to measure the specific essential work of fracture (w_e^I) in the plane-stress condition. Fig. 6 suggests that the w_e^I for ABS is 12.7 kJ/m^2.

It has been recommended [4] that the range of ligament length L_0 for metals when subjected to the plane-stress

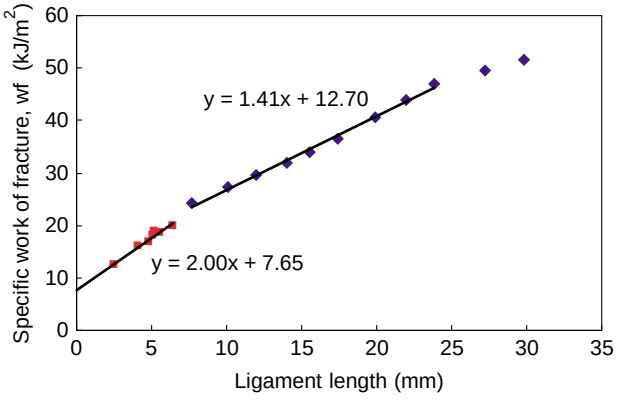

Fig. 6. Plot of specific work of fracture in mode I (w_f^I) as a function of ligament length.

condition should be:

$$(3-5)t \le L_0 \le \min\left(\frac{W}{3}, 2r_p\right) \quad (6)$$

where t is specimen thickness, W specimen width, and $2r_p$ the plastic zone size that can be determined by:

$$2r_p = \frac{Ew_e^I}{\pi\sigma_y^2} \quad (7)$$

where E is the Young's modulus and σ_y the uni-axial tensile yield strength. By substituting values of E, σ_y and w_e^I for ABS into Eq. (7), $2r_p$ was found to be around 4.0 mm that is much shorter than $W/3$ (around 30 mm for our specimens). Therefore, the condition of min($W/3$, $2r_p$) to ensure the plane-stress condition seems to be too restrictive for ABS. Our speculation is consistent with that reported for polyethylene terephthalate glycol (PETG) [33].

The data in Fig. 6 also suggest that to ensure the plane-stress condition, the upper limit of ligament length for ABS specimens should be around 25 mm that is slightly less than the other option of the upper limit, $W/3$ (30 mm for our specimens). Based on results shown in Fig. 6, we decided to use ligament lengths in the range from 8 to 24 mm for the follow-up EWF tests to determine toughness in mode I fracture. For the follow-up tests, at least five specimens were used for each ligament length at an increment of 2 mm, to ensure repeatability of the test results.

Fig. 7 presents results of the follow-up tests, in which specific work of fracture for mode I (w_f^I) is plotted as a function of the ligament length, from ABS specimens of various thickness. The w_f^I values show very good linear relationship with the change of ligament length, with little dependence on the thickness change from 2 to 6 mm. As shown in Fig. 7, the estimated w_e^I value is 13.1 kJ/m^2. The results suggest that in the thickness range from 2 to 6 mm, specimen thickness has little effect on the w_f^I values. Therefore, w_n^I in Eq. (2) must be very small, implying that the necking effect in mode I fracture of these specimens is negligible.

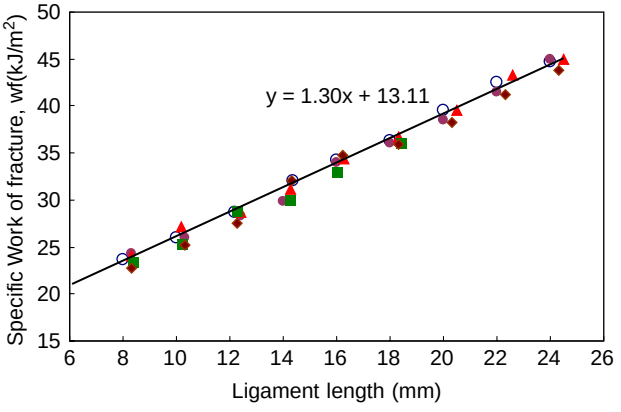

Fig. 7. Plot of specific work of fracture in mode I (w_f) as a function of ligament length with different thickness: ○, 6 mm; ○, 5 mm; ●, 4 mm; ▲, 3 mm; ◆, 2 mm.

4.2. Iosipescu test on specimens without grooves

When loaded in the Iosipescu device, specimens without grooves developed the first pair of cracks from the notch tips, which grew in a direction that was about 25° from the centre line connecting the notch tips, as shown in the circle of Fig. 8(a). The cracks opened up and grew only for a very short distance. Then, a second pair of cracks were generated nearby the tip of the first pair cracks, as shown in Fig. 8(b), in a direction about 70° from the centre line. Further loading resulted in the growth of the second pair of cracks. It should be noted that the crack development in Fig. 8 occurred around both notch tips but in the opposite direction. The asymmetric growth of the two cracks resulted in a rolling movement that eventually formed a cylinder with diameter proportional to the original ligament length, as shown in Fig. 8(c). Fig. 8(d) is a SEM micrograph of fracture surface, formed by the growth of the second crack that is indicated by an arrow in Fig. 8(c).

The above crack development process is also reflected in the load-displacement curve from the Iosipescu test. Fig. 9 shows a typical load–displacement curve from ABS specimens without the grooves, in which point A indicates the position where the first pair of cracks occurred (Fig. 8(a)) and point B the position for the second pair of cracks (Fig. 8(b)). Generation of the cracks has caused the load drop, with the rate of load drop induced by the first pair of cracks being much faster than that by the second pair of cracks.

The generation of the first pair of cracks caused a sharp drop of the load, from point A to point B in Fig. 9. The first pair of cracks are 'shear-like cracks' that were also observed by Husaini et al. [2]. Formation of the first pair of cracks can be explained by the competition of maximum principal stress and maximum shear stress [17]. The corresponding critical stresses are derived from the yielding theories (von-Mises or Tresca for ductile materials), with the concept that material yields and crack initiation occurs when either stress components reaches a critical value. It should be noted that after the crack is initiated, we believe that the mode of the following fracture process is independent of that for the crack initiation. This is based on the concept that in the crack initiation stage the fracture toughness is yet to be involved in the fracture process, and that the crack initiation is governed by the critical yielding stresses. In the following crack propagation stage, after the full development of FPZ, the fracture toughness plays a major role in the mode for the crack development. At this stage, difference of fracture toughness in the two modes of fracture is a critical factor to determine the mode of crack development [34]. It should be pointed out that crack development in the initiation stage could be very different from that in the following crack growth stage. Since the crack development can be divided into two stages, the energy consumed in the crack initiation stage should not be included in the energy consumption for the crack growth that is used to determine the fracture toughness. At present, however, mode transition in the crack development has not been thoroughly investigated, with very few parameters, such as stress triaxiality, being considered to be the cause of the mode transition [34].

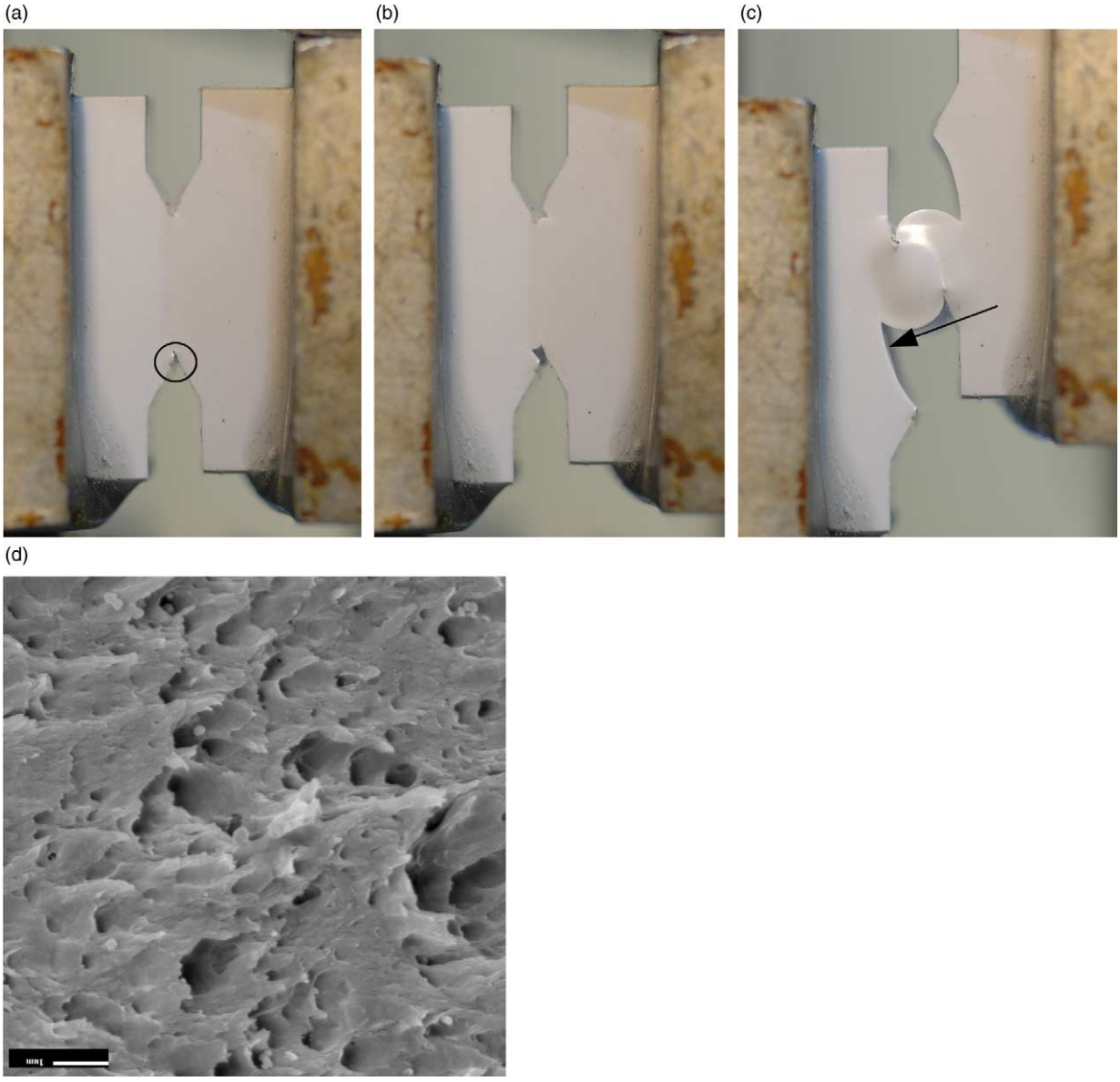

Fig. 8. Crack propagation during the Iosipescu test on specimens without the grooves: (a) first crack generation, (b) second crack generation, (c) formation of a cylinder during the crack growth, and (d) SEM micrograph taken from the fracture surface indicated by an arrow in (c).

Since the second pair of cracks are clearly visible in the fracture process presented in Fig. 8, their bifurcation angle can be used to determine the fracture mode. In our Iosipescu tests using specimens without grooves, the growth direction for the second pair of cracks is at 70° with respect to the centre line, which suggests that the second pair of cracks were generated in mode I fracture, surrounded by plastic deformation and possibly necking. The fracture surface generated by the second pair of cracks, as shown in Fig. 8(d), shows slanted torn feature that is typical for mode I fracture of ABS [35,36]. Therefore, specific essential work of fracture for mode I, w_e^I, can be determined from the Iosipescu test using the EWF concept, provided that the fracture energy for the second pair of cracks can be plotted as a function of their total length. In our attempt to determine w_e^I value from the Iosipescu test shown in Fig. 8, existence of the first pair of cracks was ignored. This was

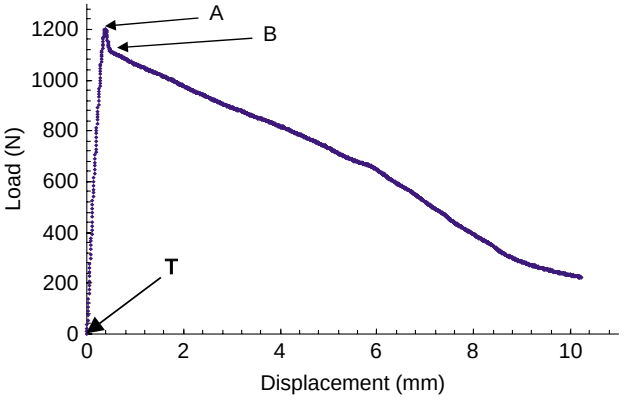

Fig. 9. Typical load-displacement curve from the Iosipescu test of ABS specimens without grooves.

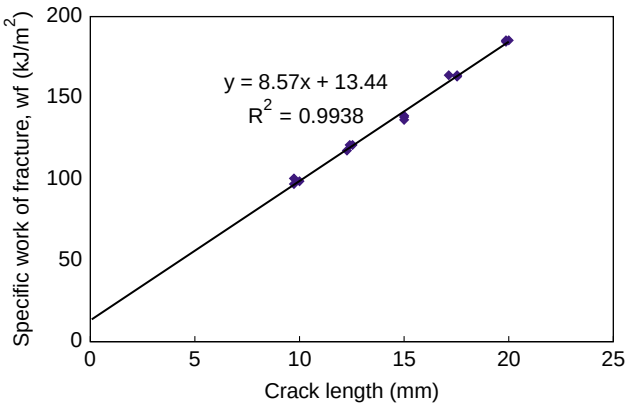

Fig. 10. Plot of specific work of fracture from Iosipescu test specimens without grooves.

deemed acceptable as the length of the first pair of cracks is very short and the corresponding fracture energy (the triangular area OAB in Fig. 9) is only a very small portion of the total fracture energy (the total area under the curve). As a result, the existence of the first pair of cracks should have little influence on the determination of the w_e^I value.

Based on the above concept, the specific work of fracture in mode I (w_f^I) for these Iosipescu tests was plotted against the arc length of the second pair of cracks, and the results are presented in Fig. 10. It should be noted that the crack length used in Fig. 10 is the true crack length for the second pair of cracks, which is about 2.5 times of the corresponding ligament length. The w_e^I value was determined to be 13.4 kJ/m^2 which is very close to the w_e^I value measured from DEN specimens under tension, 13.1 kJ/m^2. However, slope of the curve (βw_p) in Fig. 10, 8.6 kJ/m^3, is much larger than that in Fig. 7, 1.3 kJ/m^3, which suggests that the plastic work density generated in the DEN specimen in Iosipescu test is much higher than that generated in the tensile test. The steep slope in Fig. 10 yields high sensitivity of the w_e^I value to possible experimental errors. Therefore, the Iosipescu test is not recommended for the measurement of w_e^I.

4.3. Iosipescu test on specimens with grooves

V-shaped grooves, as shown in Fig. 5(b), were introduced to the specimen to generate velocity discontinuity along the ligament length direction so that the crack development is forced to be along the direction of the maximum shear stress. As stated in Section 2.4, deformation in the mode II fracture is expected to occur in the whole ligament section before crack growth commences. The initial cracking in the grooved specimens was found to be similar to that shown in Fig. 8(a), i.e. at an angle about 25° with respect to the direction of the ligament length, but resulting in much shorter crack length. This was probably due to the increase of growth resistance caused by the increase of specimen thickness in the crack growth direction. As discussed earlier, the initial cracking cannot be categorized as pure mode II fracture, and the consumed energy at this stage should not be included in the calculation of mode II fracture toughness. It should be noted that the second pair of cracks that were observed in the specimens without grooves, as shown in Fig. 8(b), did not occur in the grooved specimens. Instead, an array of multiple, short cracks were generated along the whole ligament section, as shown in Fig. 11(a). With further deformation, as shown in Fig. 11(b), the short cracks were connected to form the fracture surfaces along the ligament length. At the stage shown in Fig. 11(b), the two halves of the specimen were still connected through some fibrils that were eventually broken after extensive elongation.

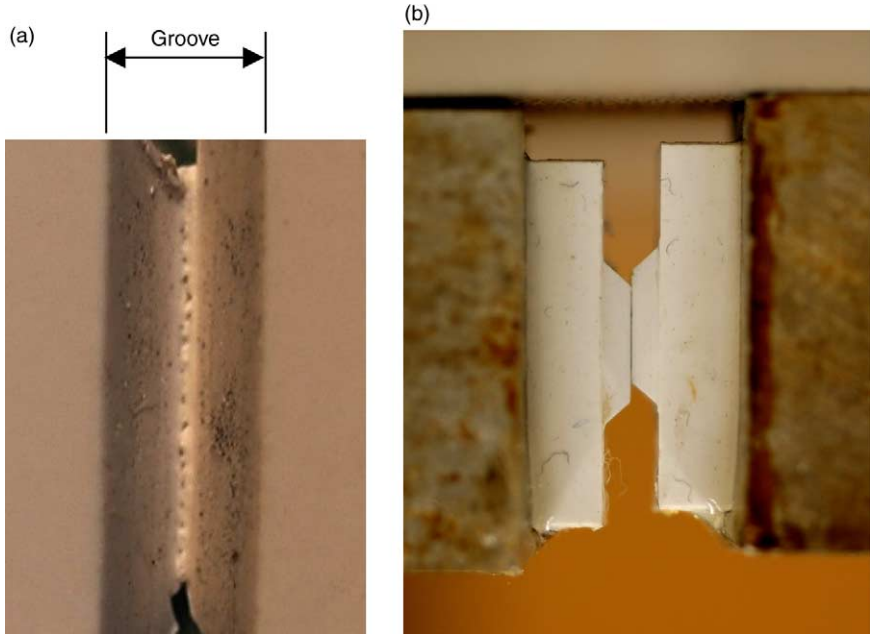

Fig. 11. Iosipescu test on the grooved specimens, showing (a) an array of cracks generated in the whole ligament section, and (b) the velocity discontinuity along the groove.

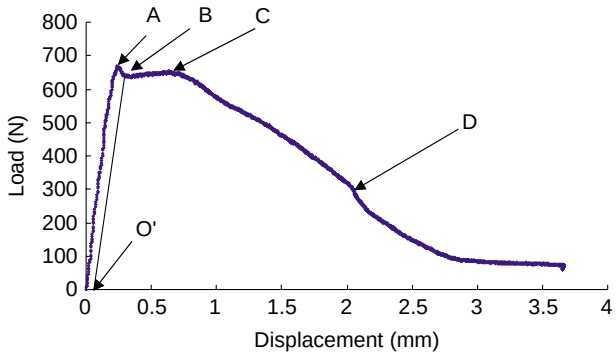

Fig. 12. A typical load–displacement curve from the Iosipescu test of the grooved specimens.

A typical load-displacement curve from the grooved DEN specimens is presented in Fig. 12 in which point A indicates the loading level for the initiation of the first pair of cracks. Advancement of the first pair of cracks stopped at point B. In the plateau region from points B to C, an array of short cracks started. Coalescence of these short cracks was reflected by a steady drop of the load in the section from C to D in Fig. 12. The section after point D was generated during the extensive elongation of the remaining fibrils, which was a deformation process after the main crack was formed, and involved mainly fibril fracture in mode I. Therefore, the deformation in the section after point D of Fig. 12 should be classified as local mode I fracture.

Based on the experimental observation, as presented in Fig. 11, the fracture development from points B to D in Fig. 12 was in the direction of the maximum shear stress with the crack evolving simultaneously in the whole ligament section, which satisfies the first and second criteria for mode II fracture (crack orientation and development of FPZ, respectively). The remaining criterion that needs to be satisfied is the work of fracture, as expressed by Eq. (4), that is, the specific work of fracture should not be a function of ligament length. This, however, requires the extraction of energy consumption from crack growth in this part of curve.

As a first attempt to extract energy consumption for mode II fracture from the Iosipescu test using the grooved DEN specimens, the energy consumption before point B in Fig. 12 was included in the calculation for the specific work of fracture, w_f. This was deemed acceptable because the curve in Fig. 12 suggests that the energy consumed before point B (0–A–B–0′ of which point O′; is slightly to the right of point O to take into account the plastic deformation) is a very small fraction of the energy consumed in the test. On the other hand, the energy consumed after point D in Fig. 12, which is for fibril fracture in mode I, is significant and should be excluded from the calculation for w_f.

Fig. 13 compares w_f values calculated using the grooved specimens. Specimens with three different groove depths, labelled in terms of the remaining specimen thickness (to be named groove thickness in the rest of the paper) were used for the comparison. Fig. 13(a), based on the total area under the curve, shows much more scattering than Fig. 13(b) that has excluded the area after point D in Fig. 12. Fig. 13(b) also indicates that with the exclusion of the area after point D in Fig. 12, the w_f values become relatively independent of the ligament length, which is consistent with the prediction by Eq. (5). The results in Fig. 13 suggest that the above approach for extraction of energy consumption for mode II fracture meets the third criterion given in Section 2.4.

Supporting evidence for mode II fracture was obtained by examining plastic deformation in the grooved specimens. All of the specimens for Fig. 13 show constrained plastic deformation that is limited to regions around the ligament section, with no indication of any size change (Fig. 4(d)) with the variation of the ligament length. However, w_f value varies with the change of groove thickness, as shown in Fig. 13(b), possibly due to the deformation energy induced by the generation of the first pair of cracks. Process to minimise this part of energy will be discussed later in this section.

Further investigation of the generation of the first pair of cracks was conducted through microscopy. A typical SEM micrograph of fracture surface from specimens for Fig. 13 is shown in Fig. 14(a). The half-elliptical shape on the right side of

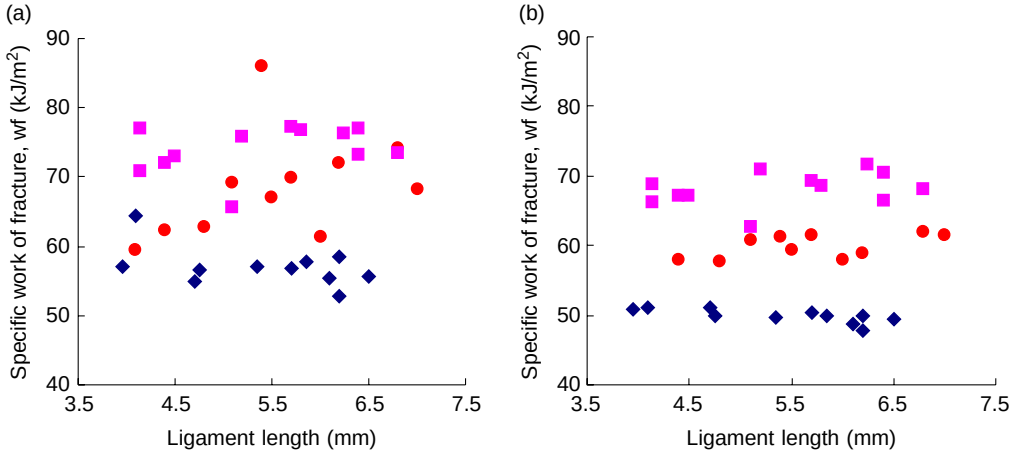

Fig. 13. Plots of the specific work of fracture (w_f) against ligament length: (a) from the total area under the curve, (b) by excluding the area covered by the curve after point D in Fig. 12. Groove thickness used is 4 mm (■), 3 mm (■), and 2 mm (♦).

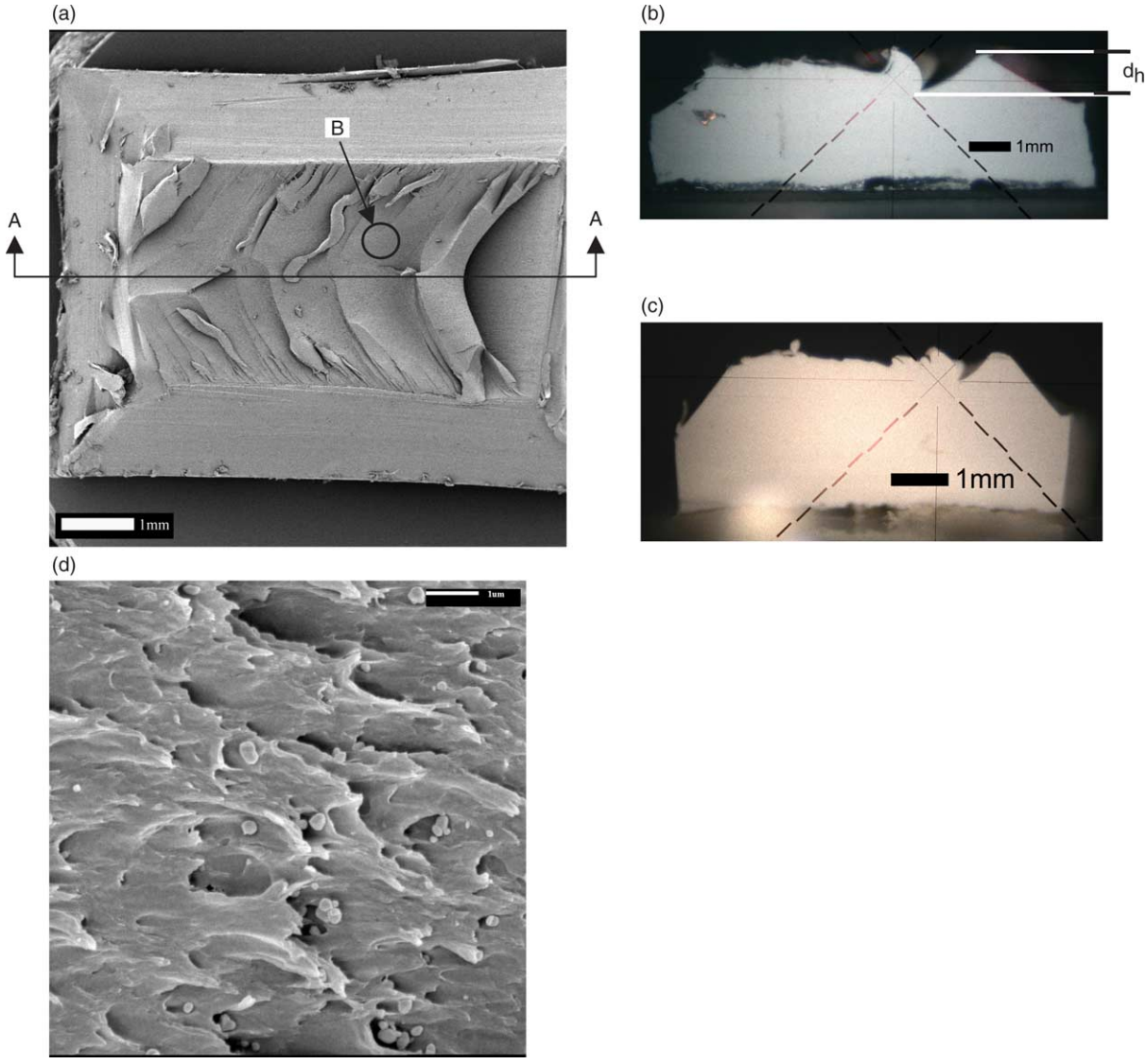

Fig. 14. (a) SEM micrograph of fracture surface from a specimen with groove thickness of 4 mm, (b) cross-sectional view along A–A in (a) for a specimen with groove thickness of 4 mm, (c) cross-sectional view for a specimen with groove thickness of 2 mm, and (d) high magnification SEM micrograph from the circular region B in (a).

the micrograph that shows crack growing into the fracture surface represents the first pair of cracks generated in the Iosipescu test. The remaining part of the fracture surface is relatively flat, containing fibrils that fractured in the last stage of the test, i.e. after point D in Fig. 12. The half-elliptical shape in Fig. 14(a) was possibly caused by the toughness variation due to the change of the deformation conditions, that is, from plane-stress-biased deformation in regions close to the edge towards the plane-strain-biased in the centre. As known in the classical mechanics [37], material deformation in a plane-stress condition yields higher toughness than that in a plane-strain condition [38]. Therefore, the growth of the first crack is deepest in the centre (along A–A in Fig. 14(a)) due to the apparent low toughness in the region, and the depth is gradually reduced towards the edges due to the increase in toughness, which leads to the formation of an elliptical contour of the fracture surface.

To examine the fracture surface topography, some of the specimens were cut along the centre line (A–A in Fig. 14(a)) and viewed using a Mitutoyo profile projector, as shown in Fig. 14(b) and (c) for groove thickness of 4 and 2 mm, respectively. The two photographs clearly suggest that the decrease of groove thickness from 4 to 2 mm has significantly reduced the growth depth of the first crack, labelled d_h in Fig. 14(b). This can also be understood from the viewpoint of transition from plane-strain to plane-stress conditions, that is, by decreasing the groove thickness, deformation in the central region is increasingly dominated by the plane-stress condition, hence raising the toughness and reducing the depth of penetration by the crack growth.

Further support to the above concept is shown in Fig. 15 in which variation of the penetration depth (d_h in Fig. 14(b)) is plotted as a function of ligament length (Fig. 15(a)) and groove thickness (Fig. 15(b)). The figures clearly show that the penetration depth is independent of the ligament length, but dependent on the groove thickness in an almost linear fashion. Therefore, by extrapolating the groove thickness to zero, plane-

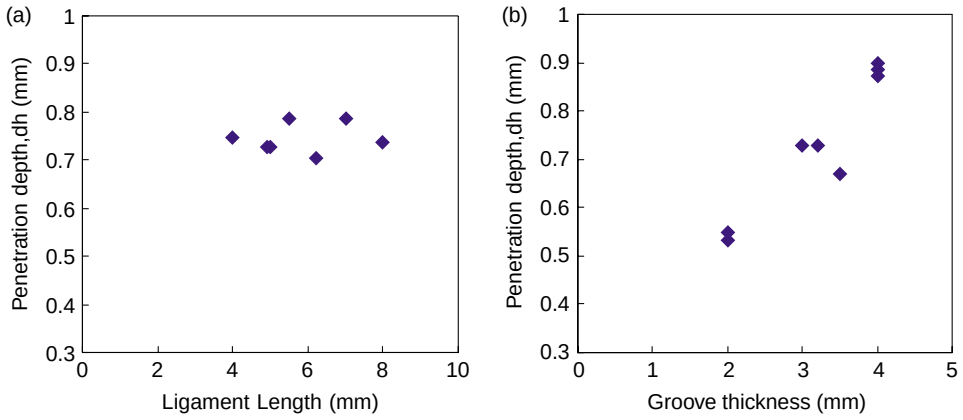

Fig. 15. Penetration depth of each of the first pair of cracks against (a) ligament length, and (b) groove thickness.

stress condition should prevail and penetration depth by the growth of the first pair of cracks should be minimised. Through this minimization process, it can be postulated that the energy consumption caused by the first pair of cracks becomes negligible for the calculation of w_f.

It may be wondered why w_f value increases with the increase of the groove thickness (Fig. 13(b)), and the increases is much bigger than the corresponding increase of the fracture energy for the generation of the first pair of cracks (area O–A–B–O′ in Fig. 12). This can be understood through the components that contribute to the fracture displacement, Δ_f, defined as the displacement at point D of Fig. 12. Fig. 16 shows Δ_f as a linear function of the groove thickness. We believe that Δ_f comes from three components:

$$\Delta_f = \Delta_{FPZ} + \Delta_f^P + \Delta_f^e \quad (8)$$

where Δ_{FPZ} is the displacement responsible for the formation of the FPZ, Δ_f^P for the plastic deformation zone and Δ_f^e for the corresponding elastic deformation. Values of Δ_{FPZ} is expected to be constant, independent of the grove thickness. Value of Δ_f^e is expected to be very small, of which variation with the change of groove thickness should be negligible. Therefore, the only component that dominates the change of Δ_f with groove thickness is Δ_f^P. With the assumption of uniform distribution of the strain inside the plastic deformation zone, the critical fracture strain in the zone (γ_f) can be expressed as the ratio of Δ_f^P to the width of the plastic deformation zone (d_P):

$$\gamma_f = \Delta_f^P / d_P \quad (9)$$

Since γ_f is expected to be constant in the range of thickness studied here, value of d_P is expected to increase with the increase of Δ_f^P. As a result, the linear increase of Δ_f (thus Δ_f^P) with the increase of the groove thickness, as shown in Fig. 16, suggests that the width of the plastic deformation zone, d_P, is proportional to the groove thickness. In other words, the role of groove thickness in the specific work of fracture in mode II (w_f^{II}) is similar to the role of the ligament length in mode I (Eq. (2)).

By excluding the energy consumed after point D in Fig. 12, as well as by extrapolating the corresponding specific work of fracture w_f to a value for zero groove thickness in order to minimize the energy consumption contributed from the generation of the first pair of cracks and that from the plastic deformation zone, the specific essential work of fracture w_e should be for the generation of shear

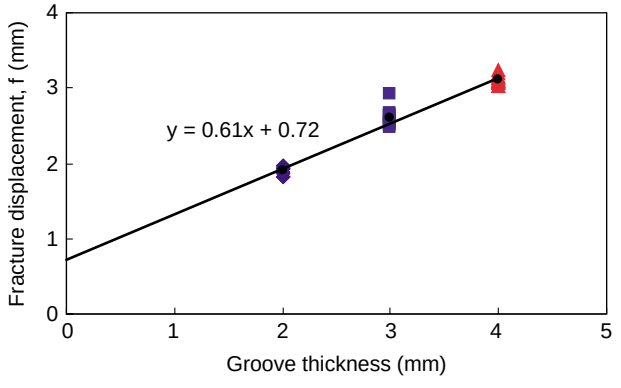

Fig. 16. Plot of the fracture displacement (Δ_f) as a function of groove thickness, using specimens of the same ligament length (5 mm), with the grooves and notches machined by a cutter of 60° in angle and 25 mm in thickness.

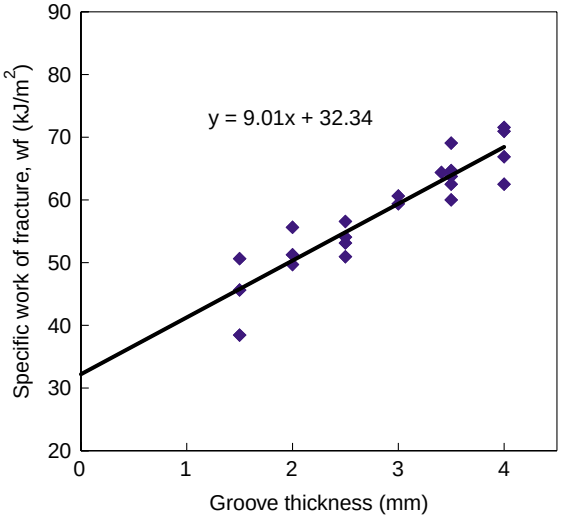

Fig. 17. Plot of the specific work of fracture (w_f) as a function of groove thickness, using specimens of the same ligament length (5 mm), with the grooves and notches machined by a cutter of 60° in angle and 25 mm in thickness.

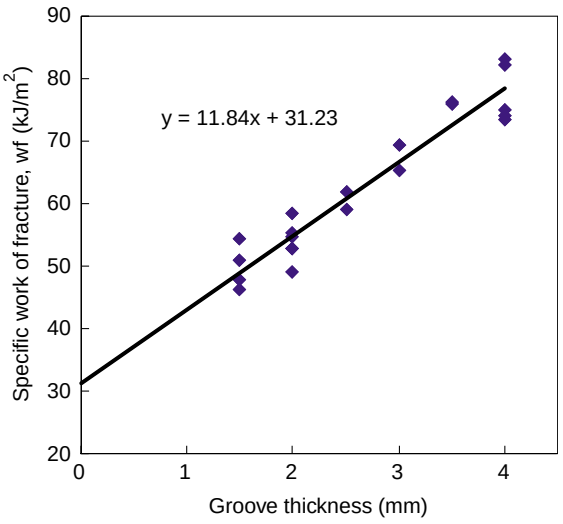

Fig. 18. Plot of the specific work of fracture (w_f) as a function of the groove thickness, using specimens of the same ligament length (5 mm) with the grooves and notches machined by a cutter of 45° in angle and 20 mm in thickness.

crack, thus representing w_e^{II}, i.e. the essential work of fracture in mode II.

Fig. 17 presents the plot using the above approach, from specimens of the same ligament length (5 mm), machined by a cutter with cutting angle of 60° and thickness of 25 mm. Linear extrapolation of the data to zero groove thickness yields w_e^{II} value of 32.3 kJ/m^2. It should be noted that deformation of these specimens met all three criteria defined in Section 2.4 for mode II fracture. Compared to the w_e^{I} value of 13.1 kJ/m^2 (Fig. 7), fracture toughness of ABS in mode II is about 2.5 times of that in mode I.

Following the report by the TC4 Committee of the European Structural Integrity Society (ESIS) [25] that the w_e^{I} value might be affected by the notch shape, additional specimens were prepared for the Iosipescu tests using a cutter of 45° in angle and 20 mm in thickness. Ligament length for these specimens was the same as that for Fig. 17, i.e. 5 mm. Results from the new set of specimens are presented in Fig. 18, with w_e^{II} value of 31.2 kJ/m^2 that is very close to that given in Fig. 17. Although further investigation may be needed before drawing a firm conclusion on the methodology for the w_e^{II} measurement, the two sets of data indicate that the change of groove angle and notch angle, both from 60 to 45°, did not have any noticeable effect on the deduced w_e^{II} value. It should be noted that although the same groove thickness and ligament length were used, the two sets of specimens for Figs. 17 and 18 showed different deflection stiffness. As a result, the data should not be grouped together to determine the value of w_e^{II}.

Some additional DEN specimens were prepared using a cutter of 90° in angle and 25 mm in thickness. But these specimens showed additional tensile cracks that were generated on the face of the notch, causing the increase of the energy consumption for the mode I fracture, thus could not be used to determine w_e^{II}.

4.4. Discussion

4.4.1. Shear fracture process

As shown in Figs. 14(d) and 8(d), the fracture surface of Iosipescu specimen with grooves shows similar features as those without grooves, but the former are slanted more closely in parallel to the fracture surface. Based on the observation of fracture development (Fig. 11) and surface topography (Fig. 14), the fracture process for the grooved DEN specimens in shear loading is proposed as follows. Firstly, an array of voids are formed along the grooves, each growing in a direction perpendicular to the maximum principal stresses, as shown in Fig. 19(a). As the deformation increases, the voids rotate and become almost parallel to the direction of cross-head movement (horizontal in Fig. 19). The cracks then emanate from the tips of the voids as shown in Fig. 19(b). Because of the geometric constraint by the grooves, the deformation occurs in a narrow region with the final fracture aligned with the grooves, as depicted in Fig. 19(c) that shows half of a fractured specimen. The similarity of Figs. 19(c) and 14(a) demonstrates the plausibility of using the proposed fracture process to

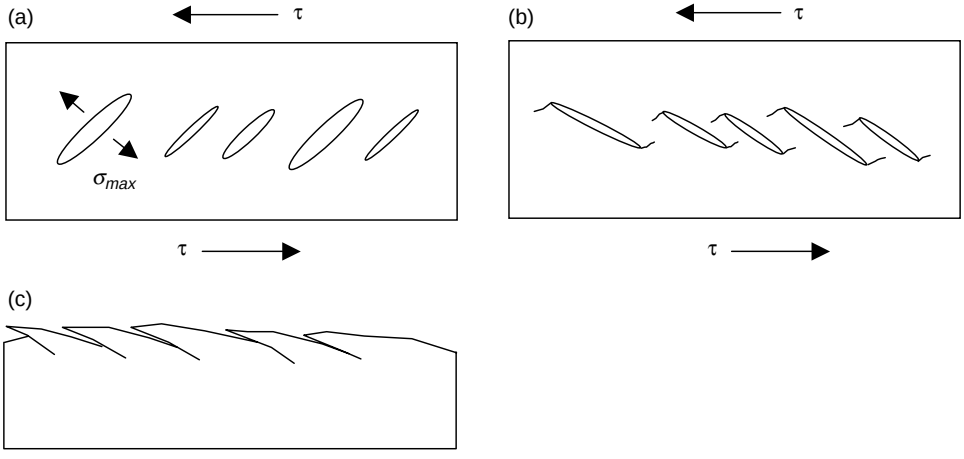

Fig. 19. Schematic representation of shear fracture process of ABS: (a) voids formation, (b) void rotation and crack emanation, and (c) side view of the surface topology.

explain the orientation of the slanted feature that is nearly parallel to the fracture surface.

4.4.2. EWF in mode II

Based on the above results, we propose a modification of Eq. (5) using the same concept for Eq. (2), to account for the dependence of w_f^{II} on the groove thickness:

$$w_f^{II} = w_e^{II} + \beta_4 w_p^{II} t_0 \quad (10)$$

where β_4 is a shape factor, t_0 the groove thickness and w_p^{II} the average plastic work density in mode II fracture. The above expression satisfies the requirement of the 3rd criterion for mode II fracture, i.e. the specific work of fracture being independent of the ligament length. Both Eqs. (2) and (10) show the thickness effect, but on different mechanisms. The change of specimen thickness in Eq. (2) affects the energy consumption for necking; while that in Eq. (10) affects the energy consumption for plastic deformation. Eq. (10) suggests that groove thickness is the main factor that affects the measured w_f^{II} value in the Iosipescu test, similar to the effect of ligament length L_0 in the DEN tensile test.

Value of w_e^{II} for mode II fracture of ABS was found to be around 32.3 kJ/m^2 that is about 2.5 times of the w_e^{I} value for mode I fracture. Such significant difference of toughness between the two fracture modes is believed to be the driving force for mode I dominating the fracture in products made of ABS.

5. Conclusions

A series of double-edge-notched Iosipescu tests were conducted to search for a means to determine the essential work of fracture in mode II, w_e^{II}. Three criteria based on physical shear deformation of polymers are proposed to identify the mode II fracture, and a test methodology based on Iosipescu device using DEN specimens with side grooves is proposed to quantify w_e^{II}.

The new test methodology yields w_e^{II} value of 32.3 kJ/m^2 for ABS, which is about 2.5 times of the corresponding value for mode I fracture, w_e^{I}, of 13.1 kJ/m^2. The significant difference of toughness is believed to be the driving force for the mode I fracture dominating the deformation in ABS products.

In contrast to the specific work of fracture in mode I, w_f^{I}, the mode II counterpart, w_f^{II}, was found to be independent of the ligament length, but showed a linear relationship with the change of the groove thickness. Based on the results, we propose an expression to correlate the essential work of fracture (w_e^{II}) with the specific work of fracture (w_f^{II}), the average plastic work density (w_p^{II}), and groove thickness (defined as the specimen thickness in the grooved cross section).

Further studies will be conducted to validate the new test methodology on the measurement of mode II fracture toughness using polymers of very different deformation characteristics. We believe that the proposed test methodology can also be applied to metallic or ceramic-based materials for the measurement of their fracture toughness in mode II. In addition to the toughness measurement, these studies will elucidate the micro-deformation mechanisms involved in the fracture process that yield significantly different toughness in the two modes of fracture.

Acknowledgements

The work was supported by Natural Sciences and Engineering Research Council of Canada (NSERC). We like to express our sincere appreciation to our colleagues, B. Faulkner and A. Yuen, for their technical support and contribution to the novel ideas in test design.

References

[1] Williams JG. Fracture mechanics of polymers. Chichester, England: Ellis Horwood Limited; 1984 p. 45 and 75.
[2] Husaini K, Kishimoto K, Notomi M, Shibuya T. Fatigue Fract Eng Mater Struct 2001;24:895–903.
[3] Li J, Zhang X-B, Recho N. Eng Fract Mech 2004;71:329–43.
[4] Cotterell B, Reddel JK. Int J Fract 1977;13:267–77.
[5] Broberg KB. Int J Fract Mech 1968;4:11.
[6] Broberg KB. J Mech Phys Solids 1971;19:407–18.
[7] Cotterell B, Pardoen T, Atkins AG. Eng Fract Mech 2005;72(6):827–48.
[8] Pardoen T, Hachez F, Marchioni B, Blyth PH, Atkins AG. J Mech Phys Solids 2004;52:423–52.
[9] Wong JSS, Ferrer-Balas D, Li RKY, Mai YW, Maspoch ML, Sue HJ. Acta Materialia 2003;51:4929–38.
[10] Iosipescu N. J Mater 1967;2(3):537–66.
[11] Sullivan JL, Kao BG, Van Oene H. Exp Mech 1984;223–32.
[12] Erdogan F, Shi GC. Basic Eng 1963;85(4):519–27.
[13] Palaniswamy K, Knauss WG. J Fract Mech 1972;8:114–7.
[14] Sih GC. Int J Fract 1974;10:305–21.
[15] Rao Q, Sun Z, Stephansson O, Li C, Btillborg B. Rock Mech Mining Sci 2003;40:355–75.
[16] Todo M, Jar P-YB, Takahashi K. Compos Sci Tech 2000;60:263–72.
[17] Chao YJ, Liu S. Int J Fract 1997;87:201–23.
[18] Pardoen T, Marchal Y, Delannay F. Eng Fract Mech 2004;69:617–31.
[19] Mai YW. Int J Mech Sci 1993;35(12):995–1005.
[20] Lauwerier HA, Koiter WT. Foundations of the theory of plasticity. Amsterdam: North-Holland Publishing Co.; 1971 p. 272–7.
[21] Hill RJ. Mech Phys Solids 1952;1:19–25.
[22] O'Brien TK. Composites 1998;29B:57–62.
[23] Broberg KB. J Mech Phys Solids 1971;19:407–18.
[24] Mai YW, Cotterell B, Horlyck R, Vigna G. Polym Eng Sci 1987;27(11):804–9.
[25] Clutton EQ. Fracture of polymers, composites and adhesives. Amsterdam: Elsevier; 1999 p. 187 [ESIS publication 27].
[26] Edward M, Rodney LT. J Compos Mater 1968;2(4):523–6.
[27] Yen SC, Craddock JN, Tech KT. Exp Tech 1988;22–5.
[28] Iosipescu N. J Mater 1967;2(3):537–66.
[29] Pindera Ma, Choksi G, Hidde JS, Herakovich CT. J Compos Mater 1987;21:1164–85.
[30] Adams DF, Walrath DE. J Compos Mater 1987;21:494–507.
[31] Tohgo K, Ishii H. Fract Mech 1992;41(4):529–40.
[32] Mai YW, Cotterell B. Int J Fract 1986;32:105–25.
[33] Ching Emma CY, Li Robert KY, Mai YW. Polym Eng Sci 2000;40(2):310–9.
[34] Sutton MA, Zhao W, Boone ML, Reynolds AP, Dawicke DS. Int J Fract 1997;83:275–90.
[35] Kwon HJ, Jar P-YB, Xia Z. J Mater Sci 2004;39:4821–8.
[36] Kwon HJ, Jar P-YB, Xia Z. J Mater Sci 2005;40:965–72.
[37] Williams JG. Fracture mechanics of polymers. Chichester, England: Ellis Horwood Limited; 1984 p. 98–9.
[38] Hertzberg RW. Deformation and fracture mechanics of engineering materials. 4th ed. New York: Wiley; 1996 p. 342–5.